Extraction of rare earth ions using thermomorphic ionic liquid: In situ spatial and temporal distribution combined with thermodynamic description

Stella Papadopoulou, Antonio de Souza Braga Neto, Isabelle Billard, Clément Cousin, Valérie Briois, Anthony Beauvois, Laurent Michot, Guillaume Mériguet, Anne-Laure Rollet, Juliette Sirieix-Plénet

Extraction of rare earth ions using thermomorphic ionic liquid: *in situ* spatial and temporal distribution combined with thermodynamic description

Stella K. Papadopoulou[a], Antonio de Souza Braga Neto[a], Isabelle Billard[b], Clément Cousin[a], Valérie Briois[c], Anthony Beauvois[c], Laurent Michot[a], Guillaume Mériguet[a], Anne-Laure Rollet[a], Juliette Sirieix-Plénet[a,*]

[a]*Sorbonne Université/CNRS, Laboratoire Physico-Chimie des Électrolytes et Nano-Systèmes Interfaciaux (PHENIX), 4 place Jussieu, Paris, France*
[b]*Université Grenoble Alpes, Université Savoie Mont Blanc, CNRS, Grenoble INP, LEPMI, Saint Martin d'Hères, France*
[c]*Synchrotron SOLEIL, L'Orme des Merisiers, Gif-sur-Yvette, France*

Abstract

Homogeneous Liquid-Liquid Extraction (HLLE) provides a valuable opportunity for recycling Rare Earth Elements (REE) by circumventing the liquid-liquid interface and avoiding the problems linked to the high viscosity of ionic liquids (IL). For optimizing these processes with the ultimate goal of implementing them at the industrial scale, it is crucial to understand the mechanisms at play at various scales. In this study, we focused on the extraction of two REE elements, La(III) and Ce(III) with an HLLE system composed of the IL [Chol][TFSI], water and betaine as the extractant. We first established the phase diagram of [Chol][TFSI]/betaine/water using ^{1}H nuclear magnetic resonance (NMR) spectroscopy. We then determined the efficiency E and distribution ratio D of the HLLE for different betaine concentrations. HLLE was modelled thermodynamically to access the most likely number of betaine molecules involved in the extraction process, which appears to be 2. Finally, we monitored *in situ* the extraction using X-ray Absorption Spectroscopy (XAS) at the K-edge of both lanthanum and cerium. It allowed us on one hand, to get some insight into the local environment around the REE, and on the other hand to measure the local concentration of REE at each position within the extraction system. In this latter process, we could evidence an accumulation of REE accumulates close to the liquid-liquid interface, a feature that was suggested by some recent simulations.

Keywords: Ionic liquids, [Chol][TFSI], homogeneous liquid liquid extraction (HLLE), EXAFS, betaine

1. Introduction

Liquid-liquid extraction (LLE) is a well-established hydrometallurgical process for the separation of metals. In conventional LLE processes, the aqueous phase that contains the metal ions is in contact with a phase composed of an organic solvent and an extractant [1, 2]. However, such a process uses large volumes of toxic and/or flammable volatile organic solvents, which raises safety and environmental issues. On these grounds, current research in the field is directed towards the development of sustainable extraction systems exhibiting high extractability. In that regard, novel extraction media such as ionic liquids (ILs), deep eutectic solvents (DES) and aqueous biphasic systems (ABS) have been assessed as potential alternatives to organic solvents [3–11]. ILs are molten salts with low melting points (below 100 °C) composed of organic cations and organic or inorganic anions.

Different combinations of cations and anions lead to ILs with varying physicochemical properties that can be used in various applications such as chemical synthesis, catalysis, separation, electrochemistry etc. As far as solvent extraction is concerned, some specific features of ILs such as negligible volatility, good thermal stability, low flammability and adjustable miscibility appear particularly appealing [6, 12]. However, due to their high viscosity, intensive mixing, shaking or heating of the system is required in order to speed up extraction. A promising way

*Corresponding author
Email address: juliette.sirieix_plenet@sorbonne-universite.fr (Juliette Siricix-Plénet)

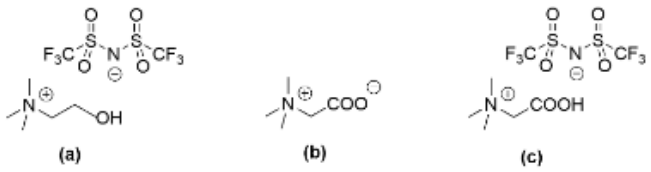

Figure 1: Chemical structure of (a) IL [Chol][TFSI], (b) extractant betaine and (c) [Hbet][TFSI]

to overcome these drawbacks is to use thermomorphic ILs that present temperature-dependent miscibility with either water [3, 13–23] or organic solvents [24–26]. Thermomorphic systems are classified as upper or lower critical solution temperature systems (UCST and LCST, respectively) based on a characteristic temperature, called critical point, above or below which the two phases are completely miscible at all compositions. When the homogeneous phase is formed, the viscosity is lowered and faster extraction equilibrium is obtained as the interface disappears. Thermomorphic systems based extraction, referred to as homogeneous liquid-liquid extraction (HLLE), has been successfully used for extracting platinum group metals, rare earth elements (REE), uranyl species and other metals [3, 13–18, 27–34]. The most extensively investigated HLLE system is the carboxyl-functionalized betainium bis(trifluoromethylsulfonyl)imide [Hbet][TFSI] with water (figure 1), classified as a UCST system (critical point equal to 55 °C for 1:1 wt/wt composition) [3, 14–16, 20, 22, 27, 30, 32]. Another widely used thermomorphic IL presenting a UCST is the choline bis(trifluoromethylsulfonyl)imide, [Chol][TFSI] (figure 1) that was used for the HLLE of Nd(III) from aqueous phases [13]. The critical point of this thermomorphic IL is 72 °C at 1:1 wt/wt composition [35]. However, pure thermorphic systems generally exhibit limited extraction performances. For that reason, the addition of extractants is often performed. For instance, zwitterionic betaine (figure 1) was added in the aqueous phase of [Hbet][TFSI], whereas hydrophobic choline hexafluoroacetylacetonate [Chol][hfac] [27, 36] was introduced in the IL phase of [Chol][TFSI] [13]. Such systems have been used for extracting various species including REE, nickel, cobalt... Still, most studies concentrate on recovery efficiency and generally do not examine in detail the phase diagram before extraction and its influence on recovery, and do not assess precisely the extraction mechanisms.

In the present work, we focus on the HLLE of two rare earth elements, La(III) and Ce(III). Both elements are in high demand due to their extensive use in numerous high-technological applications that take advantage of their unique chemical, magnetic, optical, catalytic and electrical properties [37–40]. More specifically, we analyze the HLLE of La(III) and Ce(III) using [Chol][TFSI] in combination with zwitterionic betaine as an extractant. The addition of an extractant is particularly crucial in [Chol][TFSI] that does not contain any chelating groups. Using NMR spectroscopy, we explore in detail the ternary phase diagram [Chol][TFSI]/betaine/water, which provides novel information on the reduced extraction efficiency observed for high betaine concentration. In addition, X-ray Absorption Spectroscopy (XAS) experiments were carried out for following the speciation and concentration of La and Ce during HLLE in the system [Chol][TFSI]/betaine/water.

2. Materials and methods

2.1. Chemicals

Lanthanum(III) chloride hydrate (> 99%, Prolabo), cerium(III) chloride hydrate (> 98.5%, Merck) and ultrapure water (Direct-Q 5UV Millipore) were used for preparing the aqueous phases to be extracted. Betaine (BioUltra, ≥ 99.0%), choline chloride (≥ 98.0%) and betaine hydrochloride (≥ 99.9%) were obtained from Sigma-Aldrich. High-purity grade lithium bis(trifluoromethanesufonyl)imide, LiTFSI (99.9%) was purchased from Solvionic. All reagents were used as received, without any further purification.

2.2. Synthesis of N-(2-hydroxyethyl)-N,N,N-trimethylammonium bis(trifluoromethanesufonyl)imide [Chol][TFSI]

Choline bis(trifluoromethanesufonyl)imide [Chol][TFSI] was prepared following a literature procedure [35]. LiTFSI (0.43 mol, 123.55 g) was first dissolved in water (25 mL), then added to a solution of choline chloride (0.43 mol, 60.08 g) in water (25 mL). The mixture was vigorously stirred during one hour at room temperature after which, two

phases were observed. The IL phase was then separated from the aqueous phase. To remove chloride impurities, the IL phase was washed with water until the $AgNO_3$ test was negative. The thus obtained [Chol][TFSI] was freeze-dried. The average yield was 74 %. ^{1}H NMR (500 MHz, DMSO-d6, δ ppm): 5.27 (t, 1H, -O*H*), 3.84 (m, 2H, 2 CH_2N$^+$), 3.39 (m, 2H, CH_2OH), 3.10 (s, 9H, 3 CH_3).

2.3. Synthesis of betainium bis(trifluoromethanesufonyl)imide [Hbet][TFSI]

Betainium bis(trifluoromethanesufonyl)imide [Hbet][TFSI] was synthesized according to a method described in the litterature [3]. Betaine hydrochloride (1 mol, 153.61 g) was dissolved in 250 mL of water. This solution was combined, under agitation, with 500 mL of an aqueous solution of LiTFSI (1 mol, 287.08 g). The mixture was vigorously stirred overnight one hour at room temperature after which, two phases were observed. The IL phase (bottom) was separated from aqueous phase (top) and washed several times with small deionized water quantities until the silver nitrate test no longer indicated the presence of chloride impurities. After freeze-drying, the [Hbet][TFSI] was obtained as a white solid, with a yield of 51 %. ^{1}H NMR (500 MHz, DMSO-d6, δ ppm): 4.29 (s, 2H, CH_2), 3.22 (s, 9H, 3 CH_3).

2.4. Extraction experiments

Preparation of the ionic liquid phase. According to literature, due to the mutual solubility of [Chol][TFSI] and water, the masses of the aqueous (lower) and IL (upper) phases change upon extraction. Specifically, the mass of IL phase decreases due to the migration of the IL to the aqueous phase while the mass of the aqueous phase increases [3, 27, 41]. The saturation of the IL with water before extraction experiments is therefore essential as it prevents an additional uncontrolled water uptake of IL during extraction. Furthermore, saturated [Chol][TFSI] being liquid, it can be weighed precisely and dispensed easily.

Preparation of the aqueous phase for extraction. Heptahydrated MCl_3 (where here M is La(III) or Ce(III)) water solutions with different initial metal feed concentrations were prepared : one at 100 mg/kg and another one at 1000 mg/kg. Betaine (0 to 200 mg) was then added to the metal aqueous solution (1 g) at at extractant to metal mole ratios ranging from 0 to 200. This latter ratio corresponds to a betaine concentration in the aqueous phase of 167 mg/g. Betaine concentrations were chosen based on the work of Vander Hoogerstraete et al. showing that when a large excess of betaine (compared to the concentration of Nd(III) ions) is used, the extraction equilibrium is shifted towards complex formation and high distribution ratios are obtained [3].

Extraction experiments. Extraction experiments were performed as follows: 1 g of the aqueous phase containing the metal salt solution and the extractant (upper phase) was mixed with 1 g of the IL phase containing the water saturated [Chol][TFSI] (lower phase). The mixture was then heated in an oil bath at 80 °C (above the UCST of the IL which is 72 °C [42]) and was stirred (250-300 rpm) to obtain a single homogeneous phase. When no stirring is applied at the temperature range above the UCST, formation of a homogeneous phase does not occur due to the large density difference between the two phases [3]. The time of heating above the UCST was constant for all mixtures and set at 30 min. The mixtures were then cooled down to room temperature overnight, to induce separation of two phases. Finally, the two phases were separated for analysis. The metal content in the aqueous phase was determined by inductively coupled plasma optical emission spectroscopy (ICP-OES).

Extraction efficiency can be expressed using either the distribution ratio, D or extraction percentage, $\%E$. The former can be used for the thermodynamic analysis of the extraction equilibrium, whereas the latter better describes the extraction process. The distribution ratio is defined as

$$D = \frac{[\overline{M}]}{[M]} \tag{1}$$

where $[\overline{M}]$ and $[M]$ are the equilibrium (after extraction) concentrations of the metal in the IL and aqueous phase, respectively, expressed in mg/kg.

The extraction percentage is

$$\%E = \frac{[\overline{M}]m_{IL}}{[\overline{M}]m_{IL} + [M]m_{aq}} \times 100 \tag{2}$$

where m_{IL} and m_{aq} are the masses of the IL and the aqueous phase after extraction, respectively. The metal concentration in the IL phase $[\overline{M}]$ is given by the following equation:

$$[\overline{M}] = \frac{[M]_{init} m_{aq,init} - [M] m_{aq}}{m_{IL}} \tag{3}$$

where $[M]_{init}$ and $m_{aq,\,init}$ are the metal concentration in the aqueous phase before extraction, and the mass of the aqueous phase before extraction, respectively [3]. Even after saturating the initial IL with water, small changes in the masses of both phases are observed after extraction. This is due to IL dissolving up to circa 10% of [Chol][TFSI] in water at room temperature [13]. Still, for calculating the extraction parameters (distribution ratio and extraction percentage) we considered that the mass of each phase remains unchanged and equal to the mass of the phase before extraction. It should be pointed out that this approximation leads to slightly overestimated values for the extraction parameters [3, 27].

Determination of the phase diagram for the system IL/betaine/water. For determining the phase diagram, we prepared a mixture without any metal using a protocol similar to that used in extraction experiments. At equilibrium (after heating, cooling, and phase separation) the composition of each phase in IL, betaine and water was determined by ^{1}H NMR. The mass fraction of each species w_i can be calculated with the following equation:

$$w_i = \frac{x_i M_i}{\sum_i x_i M_i} \tag{4}$$

where x_i is the mole fraction of species i and M_i its molecular weight (18, 384 and 117 g/mol for water, ionic liquid and betaine, respectively). The mole fraction x_i of the species i is then given by:

$$x_i = \frac{\frac{A_i}{n_{Hi}}}{\sum_i \frac{A_i}{n_{Hi}}} \tag{5}$$

where A_i are the integrated areas of the protons signals corresponding to species i, and n_{Hi} is the number of protons in this species.

2.5. Computing and fitting

The fitting program was written on a virtual machine implemented on a personal computer, using C++ language and the CERN fitting routine MINUIT [43]. Fit quality was assessed from the value of χ^2 expressed as :

$$\chi^2 = \frac{1}{n - N_{par}} \sqrt{\sum_{i-1}^{n} \left(D_{exp}(i) - D_{cal}(i)\right)^2} \tag{6}$$

where $D_{exp}(i)$ and $D_{cal}(i)$ are the experimental and calculated distribution ratios, respectively of point i, n the number of experimental data and N_{par} the number of free parameters.

2.6. Analysis instruments and methods

Inductive Coupled Plasma Optical Emission Spectrometry. The La(III) and Ce(III) concentrations in the aqueous phases at equilibrium were quantified using an inductively coupled plasma optical emission spectrometer (Agilent ICP-OES 5100 SVDV). A 100 µg/mL multi-element rare earth and Geo elements aqueous solution (diluted in a 5% HNO_3) (SM60A-100, VHG Labs) was used as calibration standard.

Densimetry. The densities of the aqueous and ionic liquid phases were measured at 293.15 K using an Anton Paar DMA 38 density meter.

pH measurements. pH measurements of the aqueous phases before and after extraction were performed using a sension+ PH3 pH meter (Hach) and a Sension+ 5209 pH liquid filled combination electrode for micro sample volumes (HACH).

Potentiometric titration. The concentration of chloride ions in aqueous solutions of $CeCl_3$ and $LaCl_3$ (initial aqueous phases before extraction) was determined by titration with a standard solution of $AgNO_3$ (2 mM). These aqueous solutions were then mixed with an organic IL phase saturated in water under the same experimental conditions as those used for the extractions (equal mass for the upper and the lower phase, heating of the system at 80°C under stirring for 30 min). Then the upper (aqueous phases) were separated and titrated again with silver nitrate. Results of titrations for both $CeCl_3$ and $LaCl_3$ showed that the concentration of chloride ions remains unchanged before and after extraction.

NMR. ^{1}H nuclear magnetic resonance (NMR) spectra were recorded on a 300 MHz Bruker spectrometer with a BBFO probe. 5 mm diameter NMR tubes (Wilmad, WG-1000-7) were filled with approximately 0.5 mL of each sample. In addition, a sealed capillary filled by DMSO-d6 was inserted in the NMR tube, in order to lock the signal. The sample temperature was controlled by a Bruker BCU set to 20 °C. NMR spectra were processed with the Topspin 3.6.4 program (Bruker) by performing the following steps: baseline correction, decomposition with a Lorentz/Gauss fit and integration.

X-ray Absorption Spectroscopy. X-ray absorption spectroscopy (XAS) experiments were performed at the lanthanum and cerium K edges (38925 and 40443 eV, respectively) at the ROCK Quick-EXAFS beamline of SOLEIL synchrotron (France) [44]. XAS spectra were acquired in transmission mode with three ionization chambers (Ohyo Koken) filled with a mixture of 30% Kr and 70% Ar. A first one located before the sample measured I_0, a second one located after the sample for measuring sample transmission and a third one located after thin powders of either CeO_2 or La_2O_3 that was used as internal reference for energy calibration. The monochromator used was a Si(220) quick-EXAFS channel-cut with the main Bragg-angle aligned at 4.728° with respect to X-ray and an amplitude oscillation of 0.55° allowing to cover an energy range from 38600 to 41500 eV. The channel-cut oscillates at 2 Hz allowing to record one spectrum in 250 ms. The monochromator energy was calibrated by setting the maximum of the first derivative of of a La_2O_3 pellet at 38935 eV. Harmonic rejection was ensured with Pt coated mirrors placed before and after the monochromator; and aligned at 1.9° grazing incidence with respect to the pink and monochromatic beam. The REE solutions (0.1 mol L^{-1}) in ionic liquids were recorded using specifically designed cells (see supplementary information figure S3), in order to limit the amount of dry ILs needed. The solutions were prepared in glove box under Ar and poured in the cell. The latter was directly sealed in the glove box.

In situ extraction monitoring using X-ray Absorption Spectroscopy. 1.5 g of water saturated IL was first poured in plastic vials equipped with a magnetic stirbar. Then, 1.5 g of heptahydrated $CeCl_3$ or $LaCl_3$ (0.1 mol L^{-1}), or $LaCl_3$ + $CeCl_3$ (0.05 mol L^{-1} each) water solutions and containing 150 mg of betaine were gently poured over the IL phase. Finally, the vials were introduced into an oven adapted to the beamline and placed on a magnetic stirrer operating at moderate rate. The temperature was controlled by a thermocouple close to the sample. Samples were first heated at 45°C. Once a stable temperature was obtained, stirring was stopped, and two analyses were carried out. On one hand, taking advantage of the small beam size available on ROCK (FWHM 370 µm × 300 µm horizontal × vertical), a first set of XAS spectra were recorded every 15 mm along the vertical profile of the cell. On the other hand, a second set of XAS spectra were carried out with more statistics at chosen positions in the cell, allowing to extract the EXAFS signal with a signal-to-noise ratio good enough to analyze the speciation of the metal in HLLE systems. Such a procedure was repeated for increasing temperatures (ramp 5°C/min) with continuous stirring between temperature steps (typically, 60, 70 and 80 °C). The temperature was then decreased in 10°C steps and the same experiments were carried out on each descending temperature step. Energy alignment and normalization of the quick-EXAFS data were performed using the *normal_gui* Python Graphical User Interface available at the ROCK beamline [45].

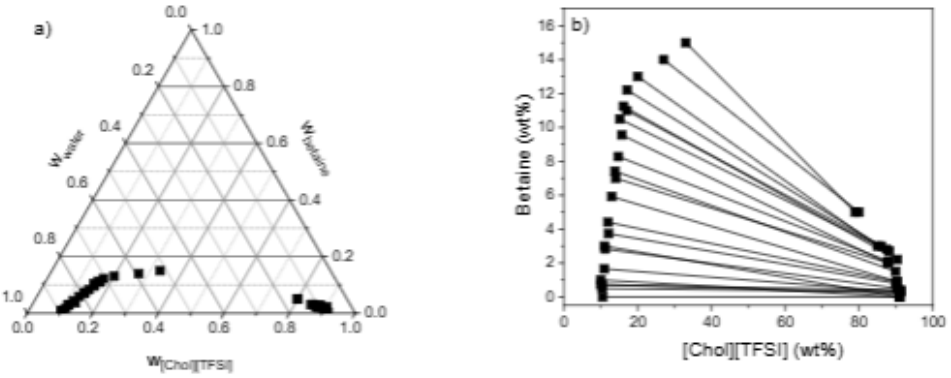

Figure 2: Phase diagrams for the system [Chol][TFSI]/betaine/water (weight fraction units) at 25 °C. a) Ternary and b) two dimensional with tie-lines

During the normalization procedure, the so-called 'edge jump' value, which is proportional to the concentration of the probed element, is obtained. This procedure consists in fitting the pre-edge region with a polynomial of degree 1 and the post-edge region with a polynomial of degree 2. The edge jump is then calculated as the difference between the value of the polynomial of degree 2 and the value of the polynomial of degree 1 at the energy of the edge (at 38 833 eV and 40 434 eV for La and Ce, respectively). Data were analyzed using *FASTOSH* software [46], applying the same extraction parameters for Ce and La. The EXAFS signals were extracted using the Autobkg algorithm (Rbkg=1.3) with *k*-weight=2. The corresponding Fourier Transforms were calculated between 3.4 and 10 $Å^{-1}$ with a Kaiser apodisation window (dk=2).

3. Results and discussion

3.1. Ternary phase diagram for the system [Chol][TFSI]/betaine/water

For properly assessing the extraction performance of HLLE systems, it is necessary to obtain an in depth understanding of the phase diagram of the mixture before metal addition. This statement is illustrated by previous studies in which the evolution of extraction efficiency with extractant concentration was not fully understood. Indeed, whereas the case of neodynium extraction in a ternary system [Hbet][TFSI] with added betaine did not reveal any significant evolution of miscibility with extractant concentration [27], the case of indium extraction in the presence of 0.01 mol L^{-1} HCl was more complex. Indeed, at high betaine concentrations the miscibility between IL and the aqueous phase was shown to increase, leading to a poor phase separation and an associated decrease of the distribution ratios [22]. To shed new light on this phenomenon, we first study the phase behavior of the ternary system [Chol][TFSI]/water/betaine through a detailed analysis of the ^{1}H NMR spectra in all the phases after phase separation (Table S1 of the SI). Figure 2 displays the ternary phase diagram (Figure 2a) and the two dimensional phase diagram relating betaine and [Chol][TFSI] (Figure 2b). It must be pointed out that in the 2D representation, some crossing of the tie-lines can be observed at high [Chol][TFSI] concentration and low betaine concentration. This unphysical behavior is related to the inaccuracy in NMR peak integration in regions where the signal of [Chol] and betaine overlap (Figure S1 and S2 in SI). Still, the ternary phase diagram thus obtained clearly shows that betaine concentration has a significant impact on the miscibility of both phases and that such an influence could be detrimental to extraction for betaine concentration as low as ≈ 20 % wt.

To test this latter conclusion, we carried out extraction experiments of La and Ce. Figure 3 presents the evolution of the extraction percentage E (Figure 3a) and distribution ratio D (Figure 3b) with betaine concentration. In the absence of added betaine, the metal recovery is low ($E < 0.2$), which confirms that [Chol][TFSI] is rather inefficient for chelating REEs. For low betaine concentrations ($\leq$ 40 mg/g), E increases rapidly with no observable difference

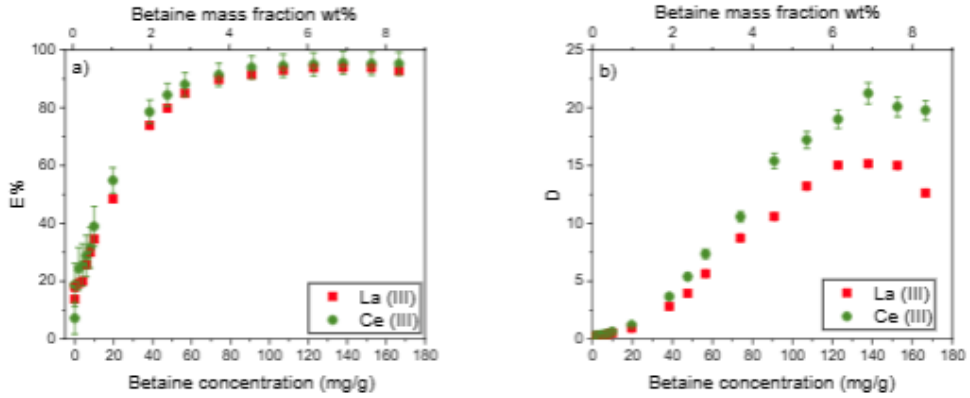

Figure 3: a) Extraction efficiency and b) distribution ratio of La(III) and Ce(III) from [Chol][TFSI] as a function of the betaine concentration in the aqueous phase or the mass fraction of betaine wt% in the extraction system

between La and Ce. E then plateaus around 97 % at high betaine concentration ($\geq$ 80 mg/g). Plotting the data as D vs betaine concentration (Figure 4b) provides additional information. Firstly, Ce leads to higher D values than La. Secondly, at high betaine concentration the two metals behave differently, Ce exhibiting a plateau whereas a decrease of D is observed for La. Such a behavior concurs with what was observed in the case of Indium extraction [22] and can be explained on the basis of the ternary phase diagram described above. Indeed, as shown in figure 4, for the composition used in the extraction experiment (blue points in figure 4), the highest betaine concentrations used are close to the boundary between the biphasic and monophasic region. In such a situation, the metal content of both phases tends to be equal, which consequently decreases the distribution ratio D. Such a conclusion was proposed as an assumption in ref. [22]. Thanks to our detailed thermodynamic study, we are able here to confirm such an assumption.

3.2. Extraction modelling

The aim of this section is to propose a plausible extraction scheme, as simple as possible, that correctly captures extraction data both qualitatively and quantitatively. Considering the results displayed in Figure 3 , it appears that even in the absence of betaine, some limited partition of Ce and La is observed. Betaine addition increases D significantly, which confirms that this species is the extractant in the system. The global distribution ratio is then the sum of that in the absence of betaine, D_0, and that only due to the presence of betaine, D_{Bet} :

$$D = D_0 + D_{\text{Bet}}. \tag{7}$$

As D_0 is directly measurable experimentally, the modelling scheme aims at determining D_{Bet}. The most common methods ("top-down") for analysing extraction data first propose an extraction chemical scheme, write the associated mathematical expressions (mass action laws, mass balance, etc.) where the unknowns are the various extraction equilibrium constants, and develop a mathematical expression for D that is fitted to experimental data. In such a procedure fit quality is highly dependent on the choice of the initial chemical scheme. Therefore, poor fit quality leads to a redefinition of the initial scheme and through successive iterations, a viable solution can be obtained. Such modelling strategy is rather tedious. For this reason, in the present study, we chose to apply an alternate strategy that can be defined as "bottom-up". In such a procedure, the envisioned chemical scheme is proposed at the end of the mathematical treatment, not at the beginning. As a starting point, any extraction equilibrium can be mathematically described through a mass action law as :

$$K = \frac{[\overline{M}]}{[M]} \prod_{j\in\text{species}} [j]^{\nu_j} \tag{8}$$

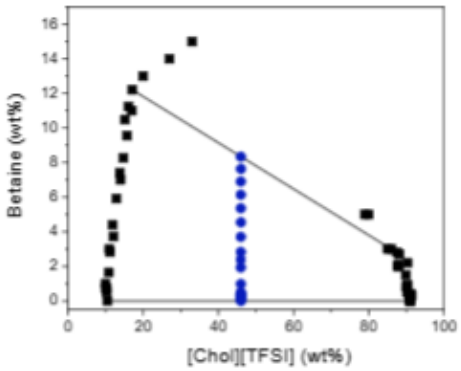

Figure 4: Experimental mass fractions of betaine (blue circles) used for the extractions of La(III) and Ce(III) from the system [Chol][TFSI]/betaine/water in the phase diagram (black squares) at 25 °C

where $[\overline{M}]$ is the concentration of the extracted metallic species in the IL phase, $[M]$ is the concentration of the metallic ion remaining in the starting phase, and j corresponds to species involved in the chemical scheme different from M and $\overline{M}$. It is then easily derived that :

$$D = \frac{[\overline{M}]}{[M]} = K\left(\prod_{j\text{:species}} [j]^{\nu_j}\right)^{-1} \tag{9}$$

In order to adapt the above equation to the problem under study, we first recall that chloride ions are not involved in the extraction mechanism (as shown from the potentiometric titration) and, as pH variation is not significant, no H^+ ions intervene in the extraction either. This reduces the number of species to be considered in equation 9. In addition, in the upper and lower phases, respectively, the amount of the $TFSI^-$ anions can be safely identified to the amount of choline cations, as the concentration of the metal ion can be neglected in comparison. This again lowers the number of possible species concentrations to be involved in equation 9. Finally, in order to reduce the number of unknown parameters to a minimum, we examined only one possible mathematical description of the extraction data of this work as:

$$D = D_0 + K\frac{[\text{Bet}]^n}{[\text{Chol}^+]^m} \tag{10}$$

It is important to stress that thanks to the binodal determination, the equilibrium concentrations of betaine and $TFSI^-$ anions are known, prior to any assumption about an extraction scheme. Therefore, the only unknown parameters of this equation are K, a scaling factor to be identified as an equilibrium extraction constant and n and m, as power coefficients, to be identified with stoechiometric coefficients, thus being integers.

Several fitting attempts have been performed, and, as is commonly observed, the mathematical function here examined presents several local minima, with χ^2 values close to one another. In the search for a plausible extraction equilibrium, we focused our study on fits for which parameter m is fixed to an integer value, while K and n are set free. From all our trials, only two fixed values of m, i.e. 3 and 6, lead to fitted n values very close to integer values, for La and Ce. Table 1 gathers these fitting results, and figure 5 displays the fitted curves, together with the experimental data.

For both La and Ce, the fits with $m = 3$ are much better than those with $m = 6$. Whatever the fixed m values, the agreement is very good for betaine concentration values lower than 100 mg/g, while the fitted curves deviate from the experimental data in the range 100-150 mg/g and display a rather satisfactory agreement above 150 mg/g. These abrupt and limited deviations of fits otherwise very satisfactory are ascribed to the experimental uncertainties

	K	n	m	χ^2
La(III)	0.23	1.93	3	0.22
	5×10^{-4}	2.98	6	0.25
Ce(III)	0.38	2.01	3	0.27
	8×10^{-4}	3.03	6	0.43

Table 1: Fitting results of equation 10 for equilibrium constant values K, stoechiometric coefficients for betaine n, and goodness of fitting χ^2 , when imposing m values

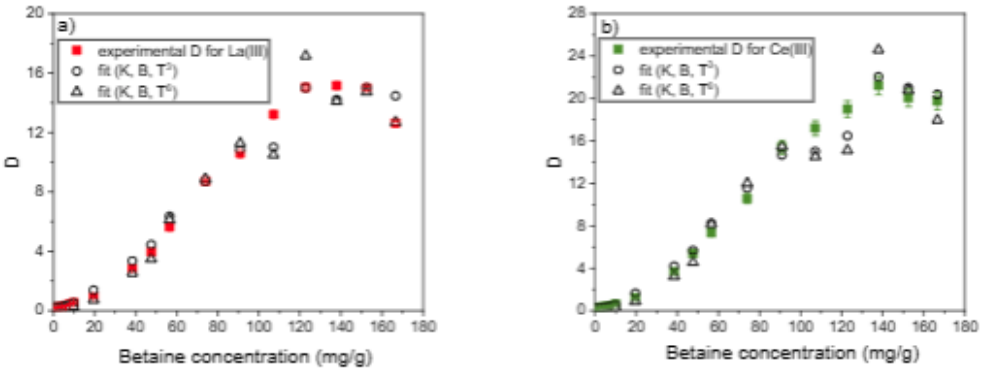

Figure 5: a) Experimental and fitted values of the distribution ratio of La(III) and b) Ce(III) from [Chol][TFSI] as a function of the betaine concentration in the aqueous phase.

of the $TFSI^-$ and betaine data, as discussed in section 3.1. The global equation scheme of the extraction can thus be expressed as:

$$M^{3+} + 2\,Bet + 3\,\overline{Chol^+} = 3\,Chol^+ + \overline{MBet_2^{3+}} \tag{11}$$

Furthermore, $\overline{Chol^+}$ being the solvent, and its activity being not significantly modified during the extraction process, one can simplify the expression of D_{Bet}:

$$D_{Bet} = K\frac{[Bet]^2[\overline{Chol^+}]^3}{[Chol^+]^3} \simeq K'\frac{[Bet]^2}{[Chol^+]^3} \tag{12}$$

3.3. In situ monitoring extraction process using localized XAS

X-ray Absorption spectroscopy can bring important information on the local environment around the rare earth. It must be underlined that XAS is a technique selective to each atom by tuning the energy range of the spectrum around the absorption edge of the atom. Hence, it is possible to follow selectively lanthanum and cerium species in the extraction of a mixture of the two metals. Furthermore, using the absorption edge jump, it is possible to determine the concentration profile of lanthanum or cerium for each temperature.

The XAS spectra have been measured as a function of the vertical position in the sample and for temperatures ranging from 30 °C to 80 °C while heating and while cooling. Typical XAS spectra are provided in SI for lanthanum and cerium at the K-edge. In addition, the XANES part of the spectra is also shown at different steps of the extraction process. As expected, there is no change in the oxidation state of the REE.

Figure 6 shows the XAS spectra of cerium at K-edge for the extraction system ($LaCl_3$ + $CeCl_3$ at 0.05 mol/L each in water with 100 mg/g of betaine/[Chol][TFSI]$_{sat}$) at 25°C before heating, at 80°C when the system is monophasic and at 25°C back after heating. For comparison, the XAS spectra of cerium in [Chol][TFSI]$_{dry}$ and [HIbet][TFSI]$_{dry}$ are also

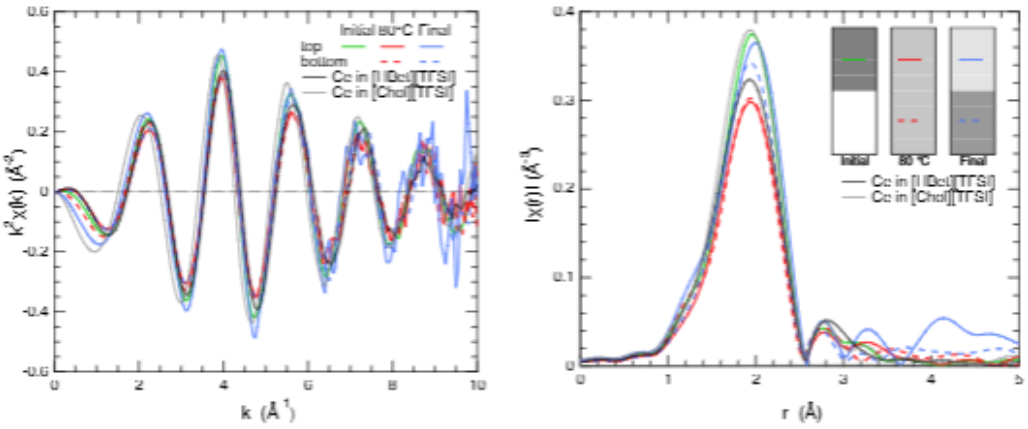

Figure 6: EXAFS signals of the cerium ions in the different phases during the extraction process compared to cerium 0.1 mol/L solutions in the ionic liquids [HBet][TFSI] and [Chol][TFSI]. *Left:* $\chi(k)$ oscillations, weighted by k^2 for Ce *Right:* Fourier Transformed Moduli $|\chi(r)|$

shown. The similar figure for the lanthanum case is given in the supplementary information (Figure S5). In view of the moderate signal-to-noise ratio in these spectra, only the first shell surrounding rare earth cations can be safely analyzed in those experiments. Many experimental and numerical studies have shown that in ionic liquids with TFSI, the metal cation (Li^+, Na^+, Ni^{2+}, Co^{2+}, Al^{3+}, etc.) is solvated by the oxygen of the TFSI anion [47–50]. In $[Chol][TFSI]_{dry}$, it has been recently shown that the OH of the choline is also involved in the solvation [51]. In aqueous solutions, La(III) and Ce(III) are surrounded by 9 water molecules in tricapped trigonal prism configuration [52, 53]. Hence, the peak observed in the radial distribution function (RDF) corresponds to oxygen atoms belonging to potentially different molecules (H_2O, $Chol^+$, $TFSI^-$, Bet and $HBet^+$). For both rare earth cations, the spectra and RDFs for the systems at 80 °C and after heating in the IL phase are close to each other, and rather similar to $[Hbet][TFSI]_{dry}$, but significantly differ from $[Chol][TFSI]_{dry}$ and room temperature initial aqueous phase. Such observations allow proposing the following scenario: At room temperature before heating, rare earth cations are surrounded by water molecules, and upon heating the system, betaine can substitute water molecules and solvate the rare earth cation. Back at room temperature, in the IL phase, betaine still solvates rare earth, whereas rare earth cations still present in the aqueous phase after the extraction process, are surrounded back by water molecules.

Such a scenario confirms the hypotheses formulated in section 3.2 about the involvement of betaine in the extraction.

In addition, the evolution of the concentrations of lanthanum and of cerium for an initial aqueous solution containing identical concentration of $LaCl_3$ and $CeCl_3$ during the extraction process has been followed (Figure 7). Prior to commenting the evolution of the concentration profiles with temperature, it must be underlined that Quick-EXAFS techniques [44] allow studying *in situ* extraction processes depending on the position within the sample, by combining a rapid acquisition of the XAS spectra (200 ms) and the spatial resolution of the synchrotron beam.

Figure 7 shows that the concentrations of both lanthanide ions exhibit similar evolutions during the process. In order to provide a clear view of what occurs in these systems, we have drawn simplified diagrams of the system in Figure 8. At the top of Figure 8, according to the measure of average concentrations in each phase, at room temperature before extraction, lanthanide ions are located in the aqueous phase, at 80°C they are homogeneously dispersed in the whole volume of the unique phase and after cooling down to room temperature, they are concentrated into the ionic liquid phase. At the bottom of Figure 8, the diagram drawn according to the value of the absorption edge jump clearly evidences a more complex behaviour. At the start of extraction, at low temperature (45°C) when the system is biphasic, the lanthanide concentration is constant in the aqueous phase from 8 mm up to the top of the cell (14 mm), and close to the interface (8 to 6 mm) the concentration decreases as deduced from Figure 7. On the other side of the interface, in the ionic liquid phase, the lanthanide concentration displays a sharp maximum near the interface (4.5 mm) followed by a decrease. This peak indicates some accumulation of the lanthanide ions at the interface. When heating up to

341 80°C, the zone in the aqueous phase where the concentration decreases becomes larger; the height of the peak in the
342 ionic liquid phase varies: its intensity increases up to 60°C then decreases. At 80°C, the two phases start merging, the
343 edge jump becomes equal all along the cell. In order to accelerate homogenisation, gentle stirring is implemented at
344 this point. The system becomes monophasic and the lanthanide ions are homogeneously distributed within the liquid.
345 Decreasing back the temperature, the system returns biphasic and the lanthanide ions are located preferentially in the
346 ionic liquid phase at the bottom of the cell. It must be noticed that there are no peaks close to the interface as what
347 was observed before HLLE.

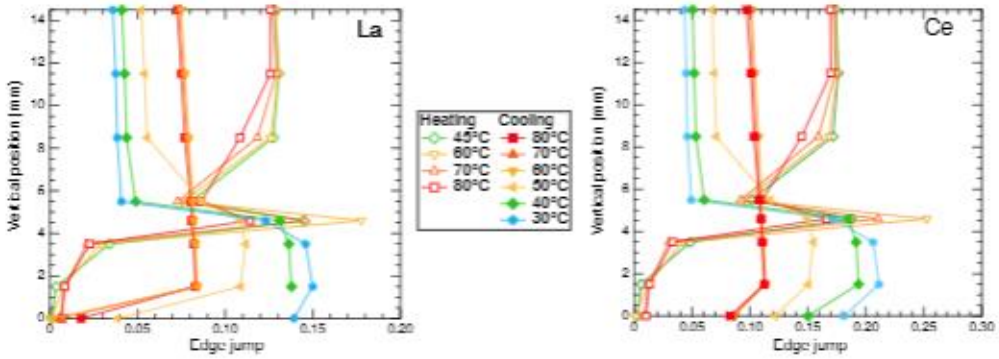

Figure 7: Evolution of the lanthanum/cerium edge jump with the vertical position in the sample during the extraction for lanthanum and cerium mixed solution, on the left for lanthanum and on the right for cerium. Note that the measurement at the very bottom of the vials is hindered leading to an underestimation of the concentration.

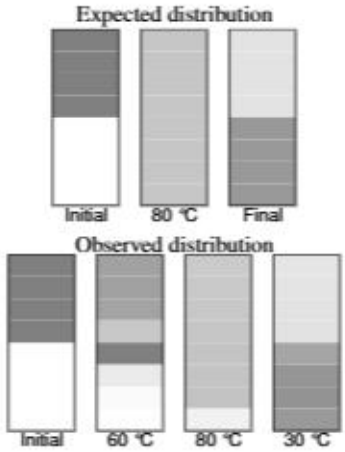

Figure 8: Diagram of the lanthanide concentration along the cell for several steps in the extraction process. *Top:* expected behaviour *Bottom:* observed distributions from XAS measurements (Figure 7)

348 The striking point here is the high value of lanthanide concentration in the vicinity of the interface in the ionic
349 liquid phase before HLLE. To the best of our knowledge, this is the first time that this phenomenon is evidenced.
350 Theoretically, such behaviour has been derived in the model proposed by Trefry et al. [54]. This model has been
351 developed for systems where a partition of a species between domains with different equilibrium concentrations and
352 diffusion coefficients can be considered. In our case, the self-diffusion coefficients of lanthanide ions are expected to
353 be much lower in the ionic liquid phase than in the aqueous phase. Even if we have not actually measured the self-

diffusion coefficient of La(III) and Ce(III) in [Chol][TFSI], data available in the literature show that the self-diffusion coefficients of added ions are about 2 orders of magnitude lower in ionic liquids [51, 55–57] than in water [58]. This is in line with the viscosity of the fluids, at 30 °C, $\eta(H_2O) \simeq 0.8$ mPa s^{-1} $\ll \eta$([Chol][TFSI]) $\simeq 80$ mPa s^{-1} and at 70 °C, $\eta(H_2O) \simeq 0.4$ mPa s^{-1} $\ll \eta$([Chol][TFSI]) $= 20$ mPa s^{-1} [59]. As a consequence, the accumulation of lanthanide ions observed in the ionic liquid phase near the interface (figure 7) may be linked to the conjunction of two phenomena: the partition equilibrium favors REE within the IL phase whereas the difference in diffusion properties between water and IL leads to some jamming at the interface. It is interesting to point out that, using molecular dynamics simulations, Mangin et al. [60] have observed an accumulation of Eu^{3+} at the interface of their LLE system. However, such simulations propose a REE layer with a thickness of about 1 nm, i.e. at a much smaller scale than what is done in the present study. Therefore, a direct comparison between both results cannot be implemented.

4. Conclusions

The liquid-liquid extraction of two rare earth cations from aqueous phase to choline-TFSI ionic liquid phase using betaine as extractant has been investigated from different points of view. First, the ternary phase diagram [Chol][TFSI]/betaine/water was established using NMR spectroscopy. Then, the extraction efficiency $\%E$ and distribution ratio D were evaluated for different betaine concentrations spanning from 0 to 170mg/g. The chosen HLLE system is clearly efficient to extract both REE, as $\%E$ exceeds 90%. However, the distribution ratio D is higher for Ce(III) (21) than La(III) (15) at the optimum betaine concentration (130 mg/g). Above this concentration of betaine, D clearly decreases for La(III) whereas it stays approximately around the same value for Ce(III). In this high betaine concentration regime, the system is close to the boundary between monophasic and biphasic state, leading to an uneven distribution of metal concentration in both phases. From these results, a modelling of the extraction mechanism was proposed. The most suitable configuration derived from such modelling suggests that rare earth is extracted with two betaine molecules. Extraction was then investigated at the molecular level and in situ using X-ray absorption spectroscopy. It confirmed the involvement of betaine in the extraction process. However, the replacement of water molecules by betaine requires energy and it is observed at 80°C. In the IL phase, rare earth cations maintain a betaine solvation shell. Furthermore, significant accumulation of rare earth at the interface prior to heating could be evidenced. Such a behavior could be assigned to differences in affinity and diffusion coefficients in the two phases.

CRediT authorship contribution statement

Stella K. Papadopoulou: Investigation, Resources, Methodology, Validation, Visualization, Writing – original draft. **Antonio de Souza Braga Neto:** Investigation, Resources. **Isabelle Billard:** Methodology, Software, Formal analysis, Writing - Original Draft, Writing - Review & Editing. **Clément Cousin:** Investigation, Resources. **Valérie Briois:** Investigation, Data curation. **Anthony Beauvois:** Data curation, Formal analysis, Writing - Review & Editing. **Laurent Michot:** Investigation, Writing – original draft, Writing - Review & Editing. **Guillaume Mériguet:** Conceptualization, Methodology, Validation, Investigation, Writing – original draft, Writing - Review & Editing, Visualization, Project administration, Funding acquisition. **Anne-Laure Rollet:** Conceptualization, Validation, Investigation, Resources, Writing – original draft, Writing - Review & Editing, Visualization, Project administration. **Juliette Sirieix-Plénet:** Conceptualization, Validation, Formal analysis, Investigation, Resources, Writing – original draft, Writing - Review & Editing, Visualization, Supervision, Project administration, Funding acquisition.

Declaration of Competing Interest

Acknowledgements

The development of the Beamline ROCK was supported by a public grant overseen by the French National Research Agency (ANR) as part of the *Investissements d'Avenir* program (ANR-10-EQPX-45). The authors would like to thank Laurent Barthe for assistance on ROCK beamline and José Gomes for the machining of XAFS cells.

References

[1] Y. A. El-Nadi, Solvent extraction and its applications on ore processing and recovery of metals: Classical approach, Sep. Purif. Rev. 46 (2017) 195–215. doi:10.1080/15422119.2016.1240085.

[2] J. R. Kumar, H.-I. Lee, J.-Y. Lee, J.-S. Kim, J.-S. Sohn, Comparison of liquid–liquid extraction studies on platinum (iv) from acidic solutions using bis (2, 4, 4-trimethylpentyl) monothiophosphinic acid, Separation and purification technology 63 (2008) 184–190.

[3] T. Vander Hoogerstraete, B. Onghena, K. Binnemans, Homogeneous liquid–liquid extraction of rare earths with the betaine—betainium bis(trifluoromethylsulfonyl)imide ionic liquid system, Int. J. Mol. Sci. 14 (2013) 21353–21377.

[4] M. Wang, Q. Wang, Y. Geng, N. Wang, Y. Yang, Gold(III) separation from acidic medium by amine-based ionic liquid, J. Mol. Liq. 304 (2020) 112735. doi:10.1016/j.molliq.2020.112735.

[5] I. Billard, Chapter 256 - ionic liquids: New hopes for efficient lanthanide/actinide extraction and separation?, in: J.-C. G. Bünzli, V. K. Pecharsky (Eds.), Including Actinides, volume 43 of *Handbook on the Physics and Chemistry of Rare Earths*, Elsevier, 2013, pp. 213–273. doi:10.1016/B978-0-444-59536-2.00003-9.

[6] M. F. Volia, E. E. Tereshatov, V. Mazan, C. M. Folden, M. Boltoeva, Effect of aqueous hydrochloric acid and zwitterionic betaine on the mutual solubility between a protic betainium-based ionic liquid and water, J. Mol. Liq. 276 (2019) 296–306. doi:10.1016/j.molliq.2018.11.136.

[7] N. N. Hidayah, S. Z. Abidin, The evolution of mineral processing in extraction of rare earth elements using liquid-liquid extraction: A review, Miner. Eng. 121 (2018) 146–157. doi:10.1016/j.mineng.2018.03.018.

[8] H. Okamura, N. Hirayama, Recent progress in ionic liquid extraction for the separation of rare earth elements, Anal. Sci. (2020) 20SAR11.

[9] N. Schaeffer, H. Passos, I. Billard, N. Papaiconomou, J. A. Coutinho, Recovery of metals from waste electrical and electronic equipment (WEEE) using unconventional solvents based on ionic liquids, Crit. Rev. Env. Sci. Technol. 48 (2018) 859–922. doi:10.1080/10643389.2018.1477417.

[10] A. R. Carreira, A. Nogueira, A. P. Crema, H. Passos, N. Schaeffer, J. A. Coutinho, Super concentrated hcl in a deep eutectic solvent as media for the integrated leaching and separation of metals from end-of-life lithium-ion batteries, Chemical Engineering Journal 475 (2023) 146374.

[11] S. J. Vargas, G. Pérez-Sánchez, N. Schaeffer, J. A. Coutinho, Solvent extraction in extended hydrogen bonded fluids–separation of pt (iv) from pd (ii) using topo-based type v des, Green Chemistry 23 (2021) 4540–4550.

[12] P. Sun, D. W. Armstrong, Ionic liquids in analytical chemistry, Anal. Chim. Acta 661 (2010) 1–16. doi:10.1016/j.aca.2009.12.007.

[13] B. Onghena, J. Jacobs, L. Van Meervelt, K. Binnemans, Homogeneous liquid–liquid extraction of neodymium(III) by choline hexafluoroacetylacetonate in the ionic liquid choline bis(trifluoromethylsulfonyl)imide, Dalton Trans. 43 (2014) 11566–11578. doi:10.1039/C4DT01340A.

[14] B. Onghena, K. Binnemans, Recovery of scandium(III) from aqueous solutions by solvent extraction with the functionalized ionic liquid betainium bis(trifluoromethylsulfonyl)imide, Ind. Eng. Chem. Res. 54 (2015) 1887–1898. doi:10.1021/ie504765v.

[15] S. Ikeda, T. Mori, Y. Ikeda, K. Takao, Microwave-assisted solvent extraction of inert platinum group metals from HNO_3(aq) to betainium-based thermomorphic ionic liquid, ACS Sustainable Chem. Eng. 4 (2016) 2459–2463. doi:10.1021/acssuschemeng.6b00186.

[16] S. Kono, H. Kazama, T. Mori, T. Arai, K. Takao, Significant acceleration of PGMs extraction with UCST-type thermomorphic ionic liquid at elevated temperature, ACS Sustainable Chem. Eng. 6 (2018) 1555–1559. doi:10.1021/acssuschemeng.7b04447.

[17] N. Wang, Q. Wang, Y. Geng, X. Sun, D. Wu, Y. Yang, Recovery of Au(III) from acidic chloride media by homogenous liquid–liquid extraction with UCST-type ionic liquids, ACS Sustainable Chem. Eng. 7 (2019) 19975–19983. doi:10.1021/acssuschemeng.9b05602.

[18] Y. Wang, S. Chen, R. Liu, L. Zhang, W. Xue, Y. Yang, Toward green and efficient recycling of Au(III), Pd(II) and Pt(IV) from acidic medium using UCST-type ionic liquid, Sep. Purif. Technol. 298 (2022) 121620. doi:10.1016/j.seppur.2022.121620.

[19] K. Sasaki, K. Takao, T. Suzuki, T. Mori, T. Arai, Y. Ikeda, Extraction of Pd(ii), Rh(iii) and Ru(iii) from HNO_3 aqueous solution to betainium bis(trifluoromethanesulfonyl)imide ionic liquid, Dalton Trans. 43 (2014) 5648–5651. doi:10.1039/C4DT00091A.

[20] I. A. Shkrob, T. W. Marin, M. P. Jensen, Ionic liquid based separations of trivalent lanthanide and actinide ions, Ind. Eng. Chem. Res. 53 (2014) 3641–3653. doi:10.1021/ie4036719.

[21] P. Davris, E. Balomenos, D. Panias, I. Paspaliaris, Selective leaching of rare earth elements from bauxite residue (red mud), using a functionalized hydrophobic ionic liquid, Hydrometallurgy 164 (2016) 125–135. doi:10.1016/j.hydromet.2016.06.012.

[22] M. F. Volia, E. E. Tereshatov, M. Boltoeva, C. M. Folden, Indium and thallium extraction into betainium bis(trifluoromethylsulfonyl)imide ionic liquid from aqueous hydrochloric acid media, New J. Chem. 44 (2020) 2527–2537. doi:10.1039/C9NJ04879K.

[23] M. Wang, Q. Wang, J. Wang, R. Liu, G. Zhang, Y. Yang, Homogenous liquid–liquid extraction of Au(III) from acidic medium by ionic liquid thermomorphic systems, ACS Sustainable Chem. Eng. 9 (2021) 4894–4902. doi:10.1021/acssuschemeng.1c00497.

[24] S. Dong, B. Zheng, Y. Yao, C. Han, J. Yuan, M. Antonietti, F. Huang, LCST-type phase behavior induced by pillar[5]arene/ionic liquid host–guest complexation, Adv. Mater. 25 (2013) 6864–6867. doi:10.1002/adma.201303652.

[25] U. Domańska, M. Laskowska, A. Marciniak, Phase equilibria of (1-ethyl-3-methylimidazolium ethylsulfate + hydrocarbon, + ketone, and + ether) binary systems, J. Chem. Eng. Data 53 (2008) 498–502. doi:10.1021/je700591h.

[26] H. R. Dittmar, W. H. Schröer, Lower critical solution temperature in the metastable region of an ionic solution in a non-polar solvent, J. Phys. Chem. B 113 (2009) 1249–1252. doi:10.1021/jp8103485.

[27] T. Vander Hoogerstraete, B. Onghena, K. Binnemans, Homogeneous liquid–liquid extraction of metal ions with a functionalized ionic liquid, J. Phys. Chem. Lett. 4 (2013) 1659–1663. doi:10.1021/jz4005366.

[28] P. Nockemann, M. Pellens, K. Van Hecke, L. Van Meervelt, J. Wouters, B. Thijs, E. Vanecht, T. N. Parac-Vogt, H. Mehdi, S. Schaltin, J. Fransaer, S. Zahn, B. Kirchner, K. Binnemans, Cobalt(II) complexes of nitrile-functionalized ionic liquids, Chem. Eur. J. 16 (2010) 1849–1858. doi:10.1002/chem.200901729.

[29] D. Dupont, K. Binnemans, Recycling of rare earths from NdFeB magnets using a combined leaching/extraction system based on the acidity and thermomorphism of the ionic liquid [Hbet][Tf_2N], Green Chem. 17 (2015) 2150–2163. doi:10.1039/C5GC00155B.

[30] T. Mori, K. Takao, K. Sasaki, T. Suzuki, T. Arai, Y. Ikeda, Homogeneous liquid–liquid extraction of U(VI) from HNO_3 aqueous solution

to betainium bis(trifluoromethylsulfonyl)imide ionic liquid and recovery of extracted U(VI), Sep. Purif. Technol. 155 (2015) 133–138. doi:10.1016/j.seppur.2015.01.045.
[31] D. Depuydt, A. Van den Bossche, W. Dehaen, K. Binnemans, Metal extraction with a short-chain imidazolium nitrate ionic liquid, Chem. Commun. 53 (2017) 5271–5274. doi:10.1039/C7CC01685A.
[32] C. Deferm, J. Luyten, H. Oosterhof, J. Fransaer, K. Binnemans, Purification of crude $In(OH)_3$ using the functionalized ionic liquid betainium bis(trifluoromethylsulfonyl)imide, Green Chem. 20 (2018) 412–424. doi:10.1039/C7GC02958F.
[33] Y. Zhang, Y. Deng, W. Guo, D. Liu, Y. Ding, Enhanced homogeneous liquid–liquid extraction for the selective recovery of Sc(III) by novel UCST-type ionic liquids, ACS Sustainable Chem. Eng. 9 (2021) 9932–9940. doi:10.1021/acssuschemeng.1c03162.
[34] K. Sasaki, T. Suzuki, T. Mori, T. Arai, K. Takao, Y. Ikeda, Selective liquid–liquid extraction of uranyl species using task-specific ionic liquid, betainium bis(trifluoromethylsulfonyl)imide, Chem. Let. 43 (2014) 775–777. doi:10.1246/cl.140048.
[35] P. Nockemann, K. Binnemans, B. Thijs, T. N. Parac-Vogt, K. Merz, A.-V. Mudring, P. C. Menon, R. N. Rajesh, G. Cordoyiannis, J. Thoen, J. Leys, C. Glorieux, Temperature-driven mixing-demixing behavior of binary mixtures of the ionic liquid choline bis(trifluoromethylsulfonyl)imide and water, J. Phys. Chem. B 113 (2009) 1429–1437.
[36] T. Vander Hoogerstraete, B. Onghena, K. J. I. J. M. S. Binnemans, Homogeneous liquid–liquid extraction of rare earths with the betaine—betainium bis (trifluoromethylsulfonyl) imide ionic liquid system, Int. J. Mol. Sci. 14 (2013) 21353–21377.
[37] Y. Baba, F. Kubota, N. Kamiya, M. Goto, Recent advances in extraction and separation of rare-earth metals using ionic liquids, J. Chem. Eng. Jpn. 44 (2011) 679–685. doi:10.1252/jcej.10we279.
[38] F. T. Edelmann, Lanthanide amidinates and guanidinates in catalysis and materials science: a continuing success story, Chem. Soc. Rev. 41 (2012) 7657–7672. doi:10.1039/C2CS35180C.
[39] R. G. Eggert, Minerals go critical, Nat. Chem. 3 (2011) 688–691. doi:10.1038/nchem.1116.
[40] K. Wang, H. Adidharma, M. Radosz, P. Wan, X. Xu, C. K. Russell, H. Tian, M. Fan, J. Yu, Recovery of rare earth elements with ionic liquids, Green Chem. 19 (2017) 4469–4493. doi:10.1039/C7GC02141K.
[41] C. Deferm, B. Onghena, T. Vander Hoogerstraete, D. Banerjee, J. Luyten, H. Oosterhof, J. Fransaer, K. Binnemans, Speciation of indium(III) chloro complexes in the solvent extraction process from chloride aqueous solutions to ionic liquids, Dalton Trans. 46 (2017) 4412–4421.
[42] D. Depuydt, L. Liu, C. Glorieux, W. Dehaen, K. Binnemans, Homogeneous liquid–liquid extraction of metal ions with non-fluorinated bis (2-ethylhexyl) phosphate ionic liquids having a lower critical solution temperature in combination with water, Chem. Commun. 51 (2015) 14183–14186.
[43] F. James, M. Roos, MINUIT - a system for function minimization and analysis of the parameter errors and correlations, Comput. Phys. Commun. 10 (1975) 343–367. doi:10.1016/0010-4655(75)90039-9.
[44] V. Briois, C. L. Fontaine, S. Belin, L. Barthe, T. Moreno, V. Pinty, A. Carcy, R. Girardot, E. Fonda, ROCK: the new quick-EXAFS beamline at SOLEIL, J. Phys. Conf. Ser. 712 (2016) 012149. doi:10.1088/1742-6596/712/1/012149.
[45] C. Lesage, E. Devers, C. Legens, G. Fernandes, O. Roudenko, V. Briois, High pressure cell for edge jumping X-ray absorption spectroscopy: Applications to industrial liquid sulfidation of hydrotreatment catalysts, Catal. Today 336 (2019) 63–73. doi:10.1016/j.cattod.2019.01.081.
[46] G. Landrot, FASTOSH: a software to process XAFS data for geochemical & environmental applications, Goldschmidt Conference series, Boston, 2018, p. 1402.
[47] M. Castriota, T. Caruso, R. G. Agostino, E. Cazzanelli, W. A. Henderson, S. Passerini, Raman investigation of the ionic liquid n-methyl-n-propylpyrrolidinium bis(trifluoromethanesulfonyl)imide and its mixture with $LiN(SO_2CF_3)_2$, J. Phys. Chem. A 109 (2005) 92–96. doi:10.1021/jp046030w.
[48] Y. Umebayashi, H. Hamano, S. Seki, B. Minofar, K. Fujii, K. Hayamizu, S. Tsuzuki, Y. Kameda, S. Kohara, M. Watanabe, Liquid structure of and Li^+ ion solvation in bis(trifluoromethanesulfonyl)amide based ionic liquids composed of 1-ethyl-3-methylimidazolium and n-methyl-n-propylpyrrolidinium cations, J. Phys. Chem. B 115 (2011) 12179–12191. doi:10.1021/jp2072827.
[49] J. M. Vicent-Luna, E. Azaceta, S. Hamad, J. M. Ortiz-Roldán, R. Tena-Zaera, S. Calero, J. A. Anta, Molecular dynamics analysis of charge transport in ionic-liquid electrolytes containing added salt with mono, di, and trivalent metal cations, ChemPhysChem 19 (2018) 1665–1673. doi:10.1002/cphc.201701326.
[50] X. Xu, L. Su, F. Lu, Z. Yin, Y. Gao, L. Zheng, X. Gao, Unraveling anion effect on lithium ion dynamics and interactions in concentrated ionic liquid electrolyte, J. Mol. Liq. 361 (2022) 119629. doi:10.1016/j.molliq.2022.119629.
[51] O. Karé, A. De Souza Braga Neto, B. Rigaud, Q. Berrod, S. Lyonnard, C. Cousin, J. Sirieix-Plénet, A.-L. Rollet, G. Mériguet, NMR investigation of multi-scale dynamics in ionic liquids containing Li^+ and La^{3+}: From vehicular to hopping transport mechanism, Journal of Ionic Liquids 4 (2024) 100087. doi:https://doi.org/10.1016/j.jil.2024.100087.
[52] I. Persson, P. D'Angelo, S. De Panfilis, M. Sandström, L. Eriksson, Hydration of lanthanoid(III) ions in aqueous solution and crystalline hydrates studied by EXAFS spectroscopy and crystallography: The myth of the "gadolinium break", Chemistry – A European Journal 14 (2008) 3056–3066. doi:10.1002/chem.200701281.
[53] P. D'Angelo, A. Zitolo, V. Migliorati, I. Persson, Analysis of the detailed configuration of hydrated lanthanoid(III) ions in aqueous solution and crystalline salts by using K- and L_3-edge XANES spectroscopy, Chem. Eur. J. 16 (2010) 684–692. doi:10.1002/chem.200900122.
[54] M. Trefry, J. Öhman, G. Davis, A simple numerical approach for assessing coupled transport processes in partitioning systems, Appl. Math. Model. 25 (2001) 479–498. doi:10.1016/S0307-904X(00)00063-9.
[55] H. P. K. Ngo, E. Planes, C. Iojoiu, P. Soudant, A.-L. Rollet, P. Judeinstein, Transport properties of alkali/alkaline earth cations in ionic-liquid based electrolytes, J. Ion. Liq. 2 (2022) 100044. doi:10.1016/j.jil.2022.100044.
[56] O. Borodin, G. A. Giffin, A. Moretti, J. B. Haskins, J. W. Lawson, W. A. Henderson, S. Passerini, Insights into the structure and transport of the lithium, sodium, magnesium, and zinc bis(trifluoromethansulfonyl)imide salts in ionic liquids, J. Phys. Chem. C 122 (2018) 20108–20121. doi:10.1021/acs.jpcc.8b05573.
[57] N. Tachikawa, N. Serizawa, Y. Katayama, T. Miura, Electrochemistry of sn(ii)/sn in a hydrophobic room-temperature ionic liquid, Electrochim. Acta 53 (2008) 6530–6534. doi:10.1016/j.electacta.2008.04.056.
[58] R. Mills, V. M. M. Lobo, Self-diffusion in Electrolyte Solutions: a critical examination of data compiled from the literature, Elsevier, Amsterdam, 1989.
[59] A. J. L. Costa, M. R. C. Soromenho, K. Shimizu, I. M. Marrucho, J. M. S. S. Esperança, J. N. C. Lopes, L. P. N. Rebelo, Density, thermal expansion and viscosity of cholinium-derived ionic liquids, ChemPhysChem 13 (2012) 1902–1909. doi:https://doi.org/10.1002/cphc.201100852.
[60] T. Mangin, R. Schurhammer, G. Wipff, Liquid–liquid extraction of the Eu(III) cation by BTP ligands into ionic liquids: Interfacial features and extraction mechanisms investigated by md simulations, J. Phys. Chem. B 126 (2022) 2876–2890. doi:10.1021/acs.jpcb.2c00488.